Electronic Supplementary Material (ESI) for Lab on a Chip.

Immuno-biosensor on a chip: a self-powered microfluidic-based electrochemical biosensing platform for point-of-care quantification of proteins

Fatemeh Haghayegh[a#], Razieh Salahandish[a,b#], Azam Zare[a], Mahmood Khalghollah[a], Amir Sanati-Nezhad[a,b,c*]

[a] BioMEMS and Bioinspired Microfluidic Laboratory, Department of Mechanical and Manufacturing Engineering, University of Calgary, Calgary, Alberta, Canada T2N 1N4
[b] Center for BioEngineering Research and Education, University of Calgary, Calgary, Alberta, Canada T2N 1N4
[c] Biomedical Engineering Graduate Program, University of Calgary, Calgary, Alberta T2N 1N4, Canada

[*]Corresponding author:
Department of Mechanical and Manufacturing Engineering, 2500 University Drive NW, Calgary, Alberta, Canada T2N 1N4; *E-mail address:* amir.sanatinezhad@ucalgary.ca
[#] These authors contributed equally

This PDF file includes:

Table S1

Figs. S1 to S4

Other Supplementary Materials for this manuscript include the following:

Video S1

Table S1. Parameters used for optimal CO_2 laser cutting.

Sheet material	Cutting power (watts)	Engraving speed (m/s)	Numbers of cutting cycles
PMMA* (1.5 mm thickness)	85	10	10
PMMA (6 mm thickness)	95	3	20
PSA#	59	30	6
NC§ fiber	38	40	3
VW† tissue fiber	36	50	2

* polymethyl methacrylate
# pressure sensitive adhesives
§ nitrocellulose
† virgin wood

S.1. Design No. 2 – Modified

Figure S1. A representation of Design No.2-Modified performance. (A) The overall representation of the chip fabricated based on Design No.2-Modified. **(B)** The performance of the chip after dispensing the sample (within 10 min period), (scale bars: 4 mm).

S.2. Microscopy characterization of various layers of the microfluidic chip

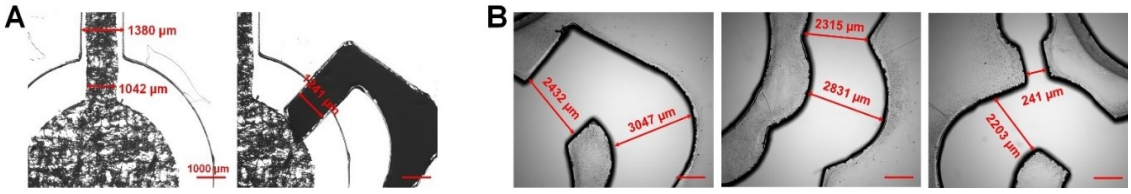

Figure S2. Optical microscopy images of fibres, pressure-sensitive adhesive (PSA), and polymethyl Methacrylate (PMMA) cut layers of the microfluidic chip. (A) Inlet channel cut inside the PSA and the VW tissue, as well as the representation of the connection point of the redox NC and the VW tissue. **(B)** Dimensions of the redox channel cut made into the 1.5 mm PMMA sheet. The soft edges of the engraved sheet depict the appropriateness of the engraving power, speed, and cutting cycles (scale bar: 1000 µm).

S3. Numerical simulation

S.3.1. Governing equations

S.3.1.1. Simulating the laminar fluid flow in the redox channel and the sensing chamber

The laminar incompressible fluid flow in the zigzag redox channel is considered as a two-phase flow with a clear interface between two immiscible liquids of fluid (the water) and the air. The dynamic of fluid flow is described by the unsteady incompressible Navier–Stokes equations. For an incompressible Newtonian fluid, continuity and momentum equations are presented in equations S1 and S2, respectively.

$$\nabla.u = 0, \quad \text{(Eq. S1)}$$

$$\rho\, \partial u/\partial t + \rho\, (u.\nabla)u = \nabla\, .\, [\, -pI + \mu\, (\, \nabla u + (\, \nabla u\,)\, \hat{}\, T\,)] + \rho g + F\_st \quad \text{(Eq. S2)}$$

where u (m/s), ρ (kg/m^3), μ (Pa.s), p (Pa) and g (m/s^2) are flow velocity vector, density, dynamic viscosity for the the water or the air, flow pressure, and gravity vector, respectively. The identity matrix is denoted by the letter I. Besides, for two-phase flow simulations, F_st is the surface tension force acting at the air-water interface. The surface tension force is calculated at the Level Set interface and is defined as:

$$F\_st = \nabla.T, \quad \text{(Eq. S3)}$$

$$T = \sigma\, (I-(nn\hat{}T\,))\, \delta, \quad \text{(Eq. S4)}$$

where,

$$n = \nabla\phi/|\nabla\phi| \quad \text{(Eq. S5)}$$

σ (N/m) is the surface tension coefficient and δ is a Dirac delta function that is nonzero at the two-phase fluid interface. The interface normal n is in terms of the level set function. The level set interface function is a smooth continuous function that is usually denoted by $0 \le \phi \le 1$. The level set function of 0.5 represents the fluid interface and ϕ equals 0 and 1 for the air and the water, respectively. For the level set method, the fluid interface between the two phases is given by:

$$\partial\phi/\partial t + u.\nabla\phi = \gamma\, \nabla.\, (\, \varepsilon\nabla\phi - \phi\, (1-\phi)\ \ \nabla\phi/|\nabla\phi|\,) \quad \text{(Eq. S6)}$$

The numerical stabilization parameters are ε and γ, where ε is interface thickness and γ is the reinitialization parameter which is equal to the maximum velocity magnitude occurring in the model. The viscosity and density of the fluids at the interface are determined as:[1]

$$\rho = \rho\_air + (\rho\_water-\rho\_air\,)\, \phi \quad \text{(Eq. S7)}$$

$$\mu = \mu\_air + (\mu\_water-\mu\_air\,)\, \phi \quad \text{(Eq. S8)}$$

S.3.1.2. The transport of diluted species

The transport of species through the water is modelled as a diffusion–convection transport equation:

$\partial c/\partial t + \nabla.(-D\nabla c) + u.\nabla c = 0$ (Eq. S9)

where c (mol/m^3) is the concentration of the species, D (m^2/s) is the diffusion coefficient, and u (m/s) is the velocity vector of the flow field obtained from coupling the physics interface to the laminar two-phase flow equations. In the transport of diluted species, two boundary conditions are considered: (1) Concentration of c = c_0 for constant concentration and (2) No flux: -n.(-D∇c) = 0. In this study, the convection-diffusion equation is solved with fluid flow equations, and diffusion of species through the well is examined until a homogeneous concentration of species is obtained on the fiber located at the surface of the sensing electrode.[2]

S.3.2. Solution domain of the redox channel

For modeling the two-phase flow through the zigzag redox channel, a computational domain is defined as shown in **Fig. S3**.

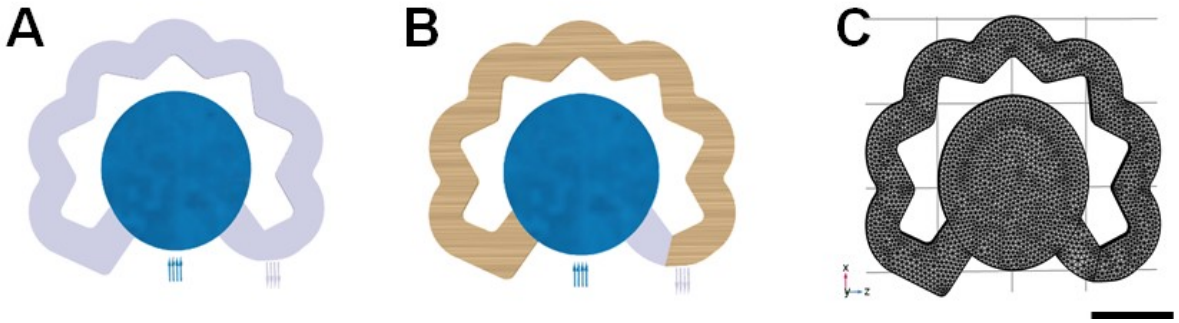

Figure S3. Solution domain of the redox channel. (A) Computational domain, **(B)** Fiber at the bottom of the zigzag redox channel, **(C)** The mesh generated for the redox channel and biosensing chamber (scale bars: 4 mm).

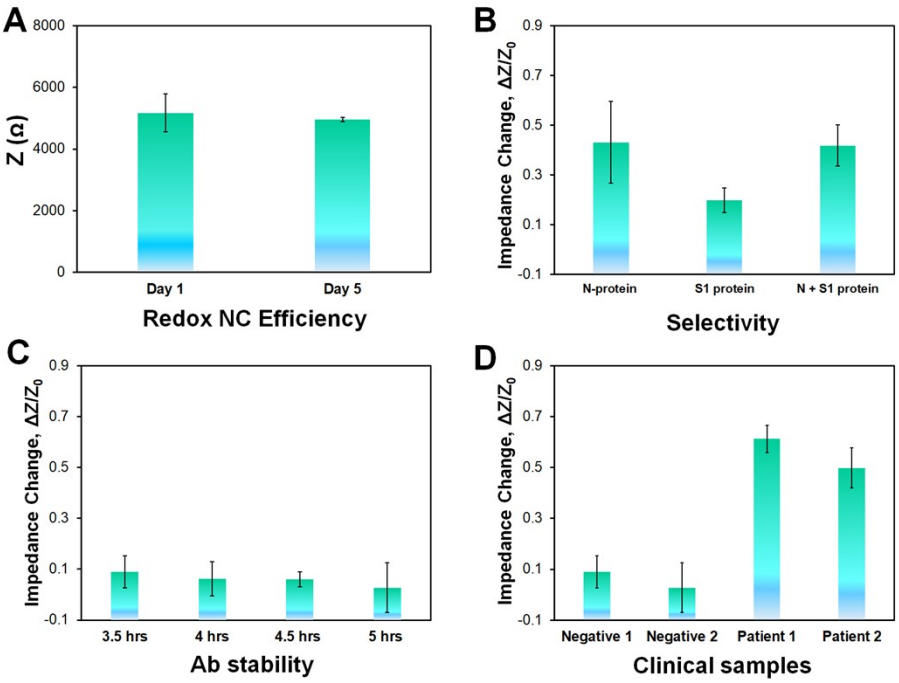

Figure S4. Characterization of the on-chip biosensing unit. (A) Evaluating the efficiency of redox-soaked NC fibers through conducting experiments on Day 1 and Day 5 of soaking in NCs. (B) Selective response of the biosensing system in its exposure to samples containing S1 proteins as opposed to the samples containing N-proteins. (C) Investigating the stability of the antibody in different time points taken out from 4 ºC by testing clinical control samples. (D) The response of the biosensing system for detecting the samples of COVID-19 positive patients and healthy control subjects (nasal samples in the universal transport medium).

Table S2. The EIS signals and the repeatability of on-chip sensing at different concentrations of N-proteins on the sensor's calibration curve.

N-Protein Concentration (pg/mL)	EIS signal (Impedance Change /$\Delta Z/Z_0$)	Standard Deviation (SD)
10	0.43	0.16
50	0.99	0.15
100	1.33	0.25
500	1.62	0.05
1000	1.90	0.32

References

1. S. Mehraji and M. Saadatmand, *Physics of Fluids*, 2021, **33**, 072009.
2. K. A. Giraldo, J. S. Bermudez, S. Torres, L. H. Reyes, J. F. Osma and J. C. Cruz, *Materials Proceedings*, 2020, **4**, 71.